Metal-Catalyzed Cyclization Reactions of Carbonyl Ylides: Synthesis and DFT Study of Mechanisms

Mehmet A. Celik, Mine Yurtsever,* Nurcan Ş. Tüzün, Füsun Ş. Güngör, Özkan Sezer, and Olcay Anaç*

Department of Chemistry, Faculty of Arts & Sciences, Istanbul Technical University, 34469 Maslak, Istanbul, Turkey

Received October 30, 2006

1,3-Dioxole derivatives were synthesized from copper(II)-catalyzed cyclization reactions of carbonyl ylides derived from 3-methylenebicyclo[2.2.1]heptan-2-one and dimethyl diazomalonate. The reaction mechanisms leading to all possible products have been extensively investigated by density functional theory. The generally accepted mechanism proposed by Doyle[12] for the carbene transformation reactions were applied to this system for the first time to shed light on the reaction mechanism and to understand the catalytic activity of $Cu(acac)_2$. Calculations have shown that the reaction mechanisms leading to different products greatly depend on the conformations of copper-stabilized carbonyl ylides, which are treated as reactants in our calculations. The conformational effects and donor−acceptor type stabilizations between the catalyst and the carbonyl ylide observed in the reactants and the transition state geometries seem to be the main reasons for the observed product selectivity. Our theoretical results are in good agreement with the experimental results, and the calculations successfully predict the experimental 75:25 product distribution.

I. Introduction

Over the past decade there has been growing interest in the use of carbonyl ylides that were simply generated by addition of carbene or carbenoids onto the oxygen atom of a carbonyl group.[1] Only a few ylides have been isolated, and their existence in reactions have been verified indirectly.[2] Thus, computational studies on these systems serve as important tools to explain the reaction mechanisms.

Among the carbonyl ylide reactions, the intra- or intermolecular 1,3-dipolar cycloadditions of carbonyl ylides with suitable dipolarophiles—an electron-deficient alkene or an aldehyde or ketone—are important strategies to obtain oxygenated heterocycles such as tetrahydrofurans,[1,3] dihydrofurans and furan derivatives,[4] and 1,3-dioxolanes,[1] which are very important intermediates for the synthesis of several natural products, possessing bioactivity.[5]

Recently, we reported the reactions of several α,β-unsaturated aldehydes and ketones having no β-alkoxy substituents and no "fixed" cisoid geometry with diazobis(carbonyl) compounds in the presence of copper(II) acetylacetonate.[6−8] In case of properly chosen *s-cis*/*E* α,β-unsaturated enones, the overall process went through 1,5-electrocyclization of the conjugated carbonyl ylide, giving dihydrofuran (Scheme 1; $R^1 = H$, path a). Furthermore, the ylides arising from (*Z*)-enones, (*E*)-enones with an R^1 substituent, and (*E*)-enals with a preference of *s-trans* conformations (Scheme 1; path b) yielded dioxole derivatives via a reaction route different from those reported by Huisgen and March[5j,9] and Doyle.[10]

In this study, the copper(II) acetylacetonate ($Cu(acac)_2$) catalyzed cycloaddition reaction of dimethyl diazomalonate (**3**) with 3-methylenebicyclo[2.2.1]heptan-2-one (**5**), a strained and cisoid-fixed bicyclic α,β-conjugated enone, was performed, and the only isolated product proved to have the 1,3-dioxole structure **7** and not the furan **6** (Scheme 2). This was in complete contrast to our previous findings, because all α,β-unsaturated ketones we experimented with ended up with dihydrofuran type products.[5−8] Product **7** actually contained two stereoisomers, **7a** and **7b**, which were inseparable in our hands. On the other hand, the crude mixture was investigated by both GC-MS and ^{1}H NMR and no evidence for a possible formation of a furan (**6**) product was found. This unusual result has led us to perform quantum-mechanical calculations on this system. Possible reaction pathways, leading to derivatives of dihydrofuran (**6**) and 1,3-dioxole (**7a** and **7b**) were studied by modeling the Cu-stabilized carbonyl ylide as a starting point in the reaction

* To whom correspondence should be addressed. E-mail: mine@itu.edu.tr (M.Y., theoretical); anac@itu.edu.tr (O.A., experimental).

(1) Padwa, A.; Hornbuckle, S. F. *Chem. Rev.* **1991**, 263−309.
(2) Janulis, E. P., Jr.; Arduengo, A. J. *J. Am. Chem. Soc.* **1983**, *105*, 5929−5930
(3) Padwa, A.; Weingarten, M. D. *Chem. Rev.* **1996**, 223−269.
(4) (a) Storm, D. L.; Spencer, T. A. *Tetrahedron Lett.* **1967**, *8*, 1865−1867. (b) Spencer, T. A.; Villarica, R. M.; Storm, D. L.; Weaver, T. D.; Friary, R. J.; Posler, J.; Shafer, P. R. *J. Am. Chem. Soc.* **1967**, *89*, 5497−5499. (c) Hodge, P.; Edwards, J. A.; Fried, J. H. *Tetrahedron Lett.* **1966**, *42*, 5175−5178.
(5) (a) Lu, C. D.; Chen, Z. Y.; Liu, H.; Hu, W. H.; Mi, A. Q.; Doyle, M. P. *J. Org. Chem.* **2004**, *69*, 4856−4859. (b) Nair, V.; Mathai, S.; Nair, S. M.; Rath, N. P. *Tetrahedron Lett.* **2003**, *44*, 8407−8409. (c) Jiang, B.; Zhang, X.; Luo, Z. *Org. Lett.* **2002**, *4*, 2453−2455. (d) Hamaguchi, M.; Matsubora, H.; Nagai, T. *J. Org. Chem.* **2001**, *66*, 5395−5404. (e) Schoop, A.; Greiving, H.; Gahrt, A. *Tetrahedron Lett.* **2000**, *41*, 1913−1916. (f) Schabbert, S.; Schaumann, E. *Eur. J. Org. Chem.* **1998**, 1873−1878. (g) Doyle, M. P.; Forbes, D. C.; Protopopova, M. N.; Stanley, S. A.; Vasbinder, M. M.; Xavier, K. R. *J. Org. Chem.* **1997**, *62*, 7210−7215. (h) Fraga, B. M. *Nat. Prod. Rep.* **1992**, *9*, 217−241. (i) Merritt, A. T.; Ley, S. V. *Nat. Prod. Rep.* **1992**, *9*, 243−287. (j) Huisgen, R.; March, R. *J. Am. Chem. Soc.* **1982**, *104*, 4953−4954.
(6) Anaç, O.; Daut, A. *Liebigs Ann. Recl.* **1997**, 1249−1254.
(7) Anaç, O.; Ozdemir, A.; Sezer, Ö. *Helv. Chim. Acta* **2003**, *86*, 290−298.
(8) Anaç, O.; Güngör, F. Ş.; Kahveci, Ç.; Cansever, M. Ş. *Helv. Chim. Acta* **2004**, *87*, 408−415.
(9) Huisgen, R.; March, R. *J. Am. Chem. Soc.* **1982**, *104*, 4952−4952.
(10) Doyle, M. P.; Russell, A. E.; Brekan, J.; Gronenberg, L. *J. Org. Chem.* **2004**, *69*, 5269−5274.

10.1021/om0609970 CCC: $37.00
Publication on Web 05/04/2007

Scheme 1. Reactions of α,β-Unsaturated Carbonyl Ylides with Dimethyl Diazomalonate in the Presence of Cu(acac)$_2$[5−8]

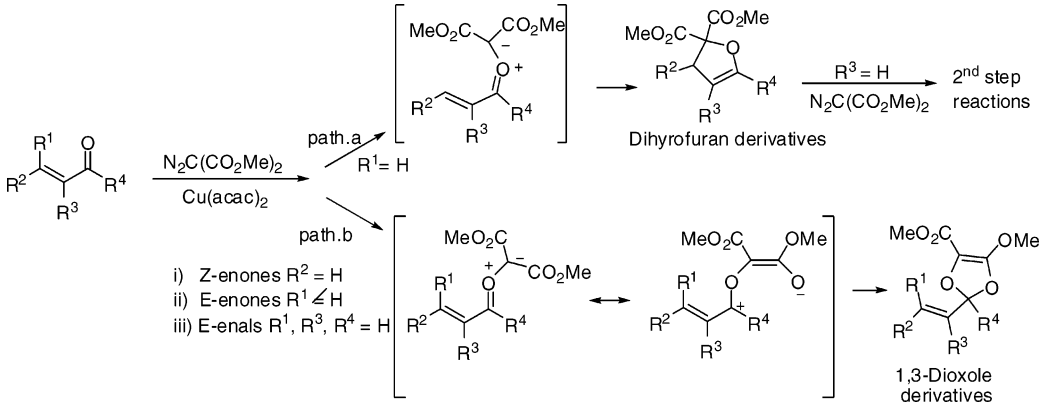

Scheme 2. Catalytic Carbene Transformation Reaction

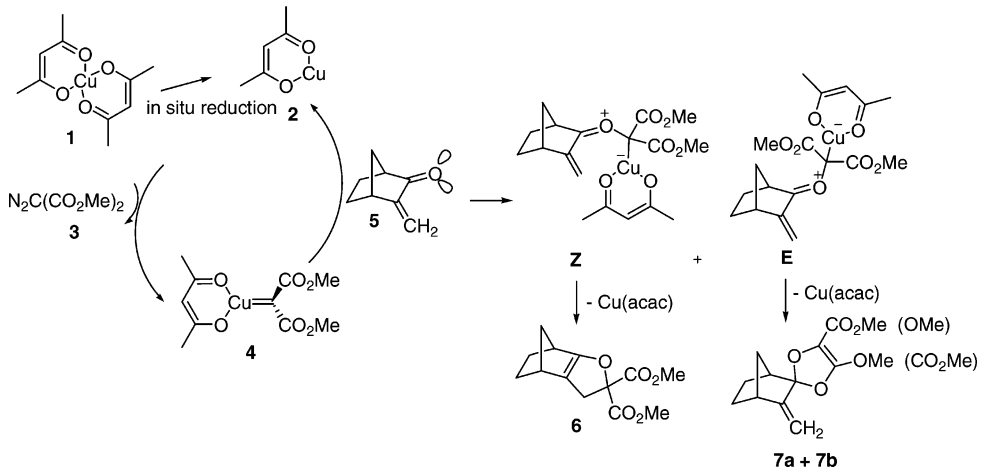

coordinate. The high selectivity can be explained by modeling the cyclization step of the metal-stabilized ylides (Scheme 2; **E** and **Z**).

In this work, copper(II) acetylacetonate, which was discovered by Nozaki and co-workers[11] in 1966, was used as the homogeneous catalyst because of its stability and the general ease of preparation and handling. The two bidentate ligands are bound to copper(II), but during diazo decomposition it is presumed that one of them dissociates to yield the active copper(I) catalyst that will produce the actual metal-stabilized carbene.[12] The proposed reaction pathway of copper-catalyzed 1,3-dipolar cycloadition reactions of carbonyl ylides proceeds in two steps: carbene complex formation and a carbene transfer reaction. First, the stable Cu(II) precatalyst **1** is reduced in situ to the active catalytic Cu(I) species **2**. Then, the diazo ester **3** reacts with **2** to give the copper(I) carbene complex **4**, the structure of which is as suggested by Doyle.[12] The reaction of the carbene complex **5** with 3-methylenebicyclo[2.1.1]heptan-2-one (**5**) produces Cu-stabilized *E* and *Z* ylides (Scheme 2). The intramolecular rearrangements of these ylides lead to five-membered oxygenated heterocycles by regenerating the catalyst **2** and possibly yielding two different products, **6** and **7**. There have been only a few reports on the spectroscopically identified copper carbene complexes in the literature.[13] Therefore, calculations on the formation and further reactivity of copper carbene complexes of this type are vital, since they will give a deeper understanding of the mechanisms and the factors affecting them. This will help experimentalists to gain more control over those kinds of reactions.

II. Computational Details

Geometry optimizations of the reactants, products, and transition states were carried out by density functional theory (DFT) methods with the empirically parametrized hybrid functional B3LYP[14] at the 6-31G(d)[15] level. Calculations were performed by using the Gaussian 03[16] software package. The equilibrium structures have been characterized by a lack of imaginary vibrations, whereas transition states have been characterized by the presence of exactly one imaginary vibration belonging to the reaction coordinate, which was also verified by the IRC[17](intrinsic reaction coordinate) analysis. The single-point electronic energies were corrected to Gibbs free energies at 298.15 K and 1 atm, on the basis of the unscaled harmonic frequencies obtained with the 6-31G(d) basis sets. The partial charges on the atoms were calculated by a natural bond orbital (NBO)[18] analysis.

(11) Nozaki, H.; Moriuti, S.; Yamabe, M.; Noyori, R. *Tetrahedron Lett.* **1966**, 59−63.

(12) Doyle, M. P.; McKervey, M. A.; Ye, T. *Modern Catalytic Methods for Organic Synthesis with Diazo Compounds*; Wiley: New York, 1998.

(13) (a) Straub, B. F.; Gruber, I.; Rominger, F.; Hofmann, P. *J. Organomet. Chem.* **2003**, *684*, 124−143. (b) Straub, B. F.; Hofmann, P. *Angew. Chem., Int. Ed.* **2001**, *40*, 1288.

(14) (a) Becke, A. D. *J. Chem. Phys.* **1993**, *98*, 1372−1377. (b) Becke, A. D. *J. Chem. Phys.* **1993**, *98*, 5648−5652. (c) Lee, C.; Yang, W.; Parr, R. G. *Phys. Rev. B* **1988**, *37*, 785−789.

(15) (a) Ditchfield, R.; Hehre, W. J.; Pople, J. A. *J. Chem. Phys.* **1971**, *54*, 724−728. (b) Hehre, W. J.; Ditchfield, R.; Pople, J. A. *J. Chem. Phys.* **1972**, *56*, 2257−2261. (c) Hariharan, P. C.; Pople, J. A. *Theor. Chim. Acta* **1973**, *28*, 213−222.

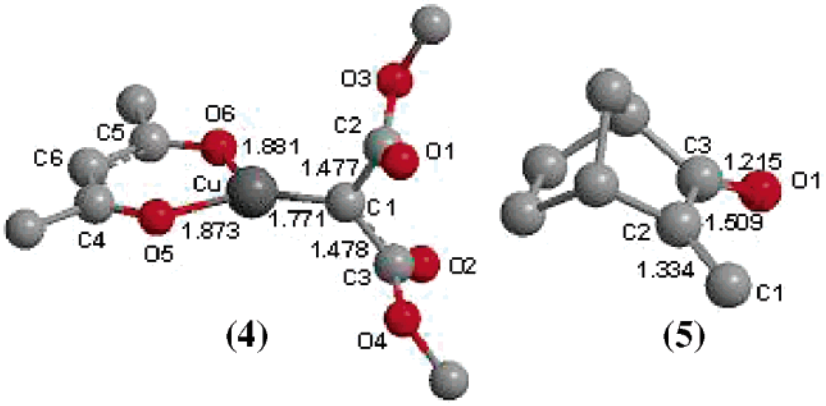

Figure 1. Optimized geometries of the molecules **4** and **5** (B3LYP/6-31G*; hydrogens are not shown).

III. Results and Discussion

To explain the experimentally observed selectivity, calculations have been performed on all the substrates that are involved in the reaction mechanisms depicted in Scheme 2.

The optimized structures of **4** and **5** and their geometrical parameters are given in Figure 1.

The molecule **2** in Scheme 2 serves as a catalytically active complex for diazo decomposition and 1,3-dipolar cycloadition reactions. It is formed by the loss of an acetylacetonate from $Cu(acac)_2$ (**1**) and becomes a catalytically active copper(I) species with the diazo reagent. The Cu−C bond length in the copper(I) carbene complex **4** is computed to be 1.771 Å, which is the shortest bond length that has been reported in the literature.[19] The bond between copper and the carbon has a strong double-bond character because of the highly electrophilic nature of the carbene, due to the electron-withdrawing groups attached to it. The back-donation occurs from the metal's d orbitals to the carbene carbon, leading to a strong π bond localization at the copper center (66.60%) with 7.55% s, 0.58% p, and 91.86% d character found from NBO analysis. The contribution from the carbene carbon is mainly by its p orbital (97.18%). The σ bond is a dative bond formed by the donation of the lone-pair electrons of the singlet carbene fragment (85.84% carbon character with 24.49% s and 75.51% p contribution) to the copper fragment (14.16% copper character with 14.28% d, 85.17% s, and 0.55% p contribution). The carbene carbon is sp^2 hybridized (the C1−C2 bond has 36.6% s and 63.4% p character and, similarly, the C1−C3 bond has 36.6% s and 63.3% p character), but it slightly deviates from the ideal sp^2 symmetry. In summary, the copper(I) carbene complex **4** can be considered as a Fischer type carbene due to the strong Cu−C π interaction. The plane of the sp^2 carbene carbon center lies orthogonal to the plane of the acetylacetonate. The $3d_{xz}$ orbital of the copper(I) accepts electrons from the oxygen ligands and then interacts with the $2p_x$ orbital of the carbene carbon atom. The carbene complex is chiral, since it has only one C_2 symmetry axis because of the trans arrangement of the C═O groups.

Scheme 3. *E* and *Z* Conformers Arising from the Reaction of 4 with 5

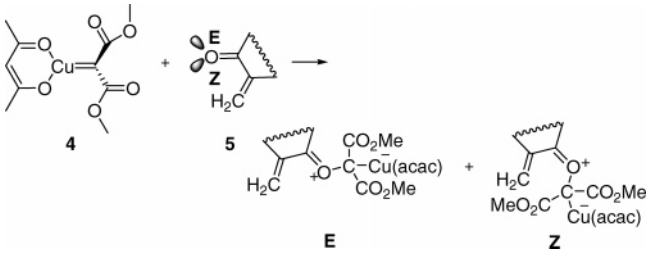

The reaction of carbene complex **4** with 3-methylenebicyclo-[2.1.1]heptan-2-one (**5**) may yield copper-stabilized ylides of two types, **E** and **Z**, as shown in Scheme 3. These two conformers are formed by the reaction of the carbene carbon with different lone pairs of oxygen. As will be explained later, the reaction mechanism of the experimentally observed product only proceeds via the **E** ylide, which is found to be 7.1 kcal/mol more stable than the **Z** ylide. Dihydrofuran formation can only happen via the Z-ylide. For this reason, an alternative path leading to the dihydrofuran derivative is studied for further comparisons.

1. Dioxole Formation. The gas chromatographic analysis in combination with the mass spectra of products that have been obtained from the reaction discussed herein showed two stereoisomers of **7**, **7a** and **7b**, which could not be separated. The isomer pair is present in a ratio of 75:25 (by GC), which gave identical mass spectra. The NMR analysis of the product revealed that it possessed the dioxole structure **7**, evidenced by the methylidene signals around 4.6−4.9 ppm.

(16) Frisch, M. J.; Trucks, G. W.; Schlegel, H. B.; Scuseria, G. E.; Robb, M. A.; Cheeseman, J. R.; Montgomery, J. A., Jr.; Vreven, T.; Kudin, K. N.; Burant, J. C.; Millam, J. M.; Iyengar, S. S.; Tomasi, J.; Barone, V.; Mennucci, B.; Cossi, M.; Scalmani, G.; Rega, N.; Petersson, G. A.; Nakatsuji, H.; Hada, M.; Ehara, M.; Toyota, K.; Fukuda, R.; Hasegawa, J.; Ishida, M.; Nakajima, T.; Honda, Y.; Kitao, O.; Nakai, H.; Klene, M.; Li, X.; Knox, J. E.; Hratchian, H. P.; Cross, J. B.; Bakken, V.; Adamo, C.; Jaramillo, J.; Gomperts, R.; Stratmann, R. E.; Yazyev, O.; Austin, A. J.; Cammi, R.; Pomelli, C.; Ochterski, J. W.; Ayala, P. Y.; Morokuma, K.; Voth, G. A.; Salvador, P.; Dannenberg, J. J.; Zakrzewski, V. G.; Dapprich, S.; Daniels, A. D.; Strain, M. C.; Farkas, O.; Malick, D. K.; Rabuck, A. D.; Raghavachari, K.; Foresman, J. B.; Ortiz, J. V.; Cui, Q.; Baboul, A. G.; Clifford, S.; Cioslowski, J.; Stefanov, B. B.; Liu, G.; Liashenko, A.; Piskorz, P.; Komaromi, I.; Martin, R. L.; Fox, D. J.; Keith, T.; Al-Laham, M. A.; Peng, C. Y.; Nanayakkara, A.; Challacombe, M.; Gill, P. M. W.; Johnson, B.; Chen, W.; Wong, M. W.; Gonzalez, C.; Pople, J. A. *Gaussian 03*, revision C.02; Gaussian, Inc.: Wallingford, CT, 2004.

(17) (a) Gonzalez, C.; Schlegel, H. B. *J. Phys. Chem.* **1990**, *94*, 5523−5527. (b) Gonzalez, C.; Schlegel, H. B. *J. Chem. Phys.* **1989**, *90*, 2154−2161.

(18) (a) Foster, P.; Weinhold, F. *J. Am. Chem. Soc.* **1980**, *102*, 7211−7218. (b) Reed, A.; Weinhold, E. F. *J. Chem. Phys.* **1983**, *78*, 4066−4073. (c) Reed, A. E.; Weihstock, R. B.; Weinhold, F. *J. Chem. Phys.* **1985**, *83*, 735−746. (d) Reed, A. E.; Weinhold, F. *J. Chem. Phys.* **1985**, *83*, 1736−1740. (e) Reed, A. E.; Curtiss, L. A.; Weinhold, F. *Chem. Rev.* **1988**, *88*, 899−926.

(19) (a) Badiei, Y. M.; Warren, T. H. *J. Organomet. Chem.* **2005**, *690*, 5989−6000. (b) Dai, X.; Warren, T. H. *J. Am. Chem. Soc.* **2004**, *126*, 10085−10094. (c) Mankad, N. P.; Gray, T. G.; Laitar, D. S.; Sadighi, J. P. *Organometallics* **2004**, *23*, 1191−1193. (d) Suenobu, K.; Itagaki, M.; Nakamura, E. *J. Am. Chem. Soc.* **2004**, *126*, 7271−7280. (e) Fraile, J. M.; Garcia, J. I.; Martinez-Merino, V.; Mayoral, J. A.; Salvatella, L. *J. Am. Chem. Soc.* **2001**, *123*, 7616−7625. (f) Boehme, C.; Frenking, G. *Organometallics* **1998**, *17*, 5801−5809.

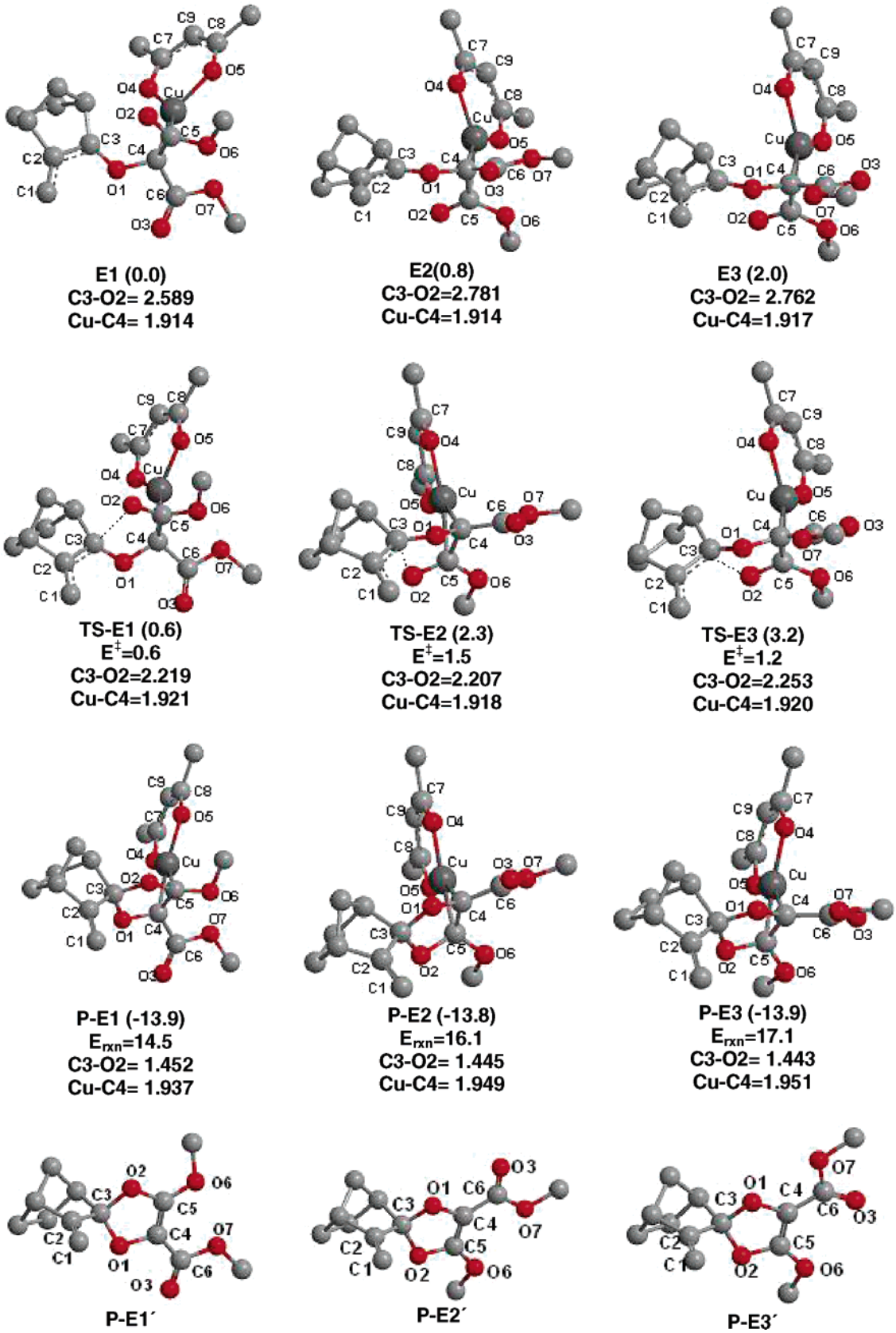

Figure 2. Optimized geometries of the (*E*)-ylides, their transition-state geometries, and the products. Relative electronic energy differences with respect to **E1** (in parentheses), activation energies, and reaction energies (E_{rxn}) are given in kcal/mol; bond distances are given in Å.

The B3LYP/6-31G(d) geometry optimizations of (*E*)-ylides revealed three conformers of similar energies (Figure 2; **E1**−**E3**). Higher energy conformers of (*E*)-ylides in addition to the global minimum are considered to have different starting geometries that lead to products **7a** and **7b**.

The **E1** ylide coordinates to the C4−C5 bond, so that it completes its fourth coordination by approaching the carbonyl group. The NBO analysis of **E1** has shown that the stabilization from the C5−O2 bond to copper and back-donation of the copper to the same bond are 8.33 and 18.5 kcal/mol, respec-

tively. The C5−O2 bond is stretched in such a way that the closing centers O2−C3 approach each other, giving a favorable geometry for the ring closure. Although the stabilization energies of σ donation coming from the lone pairs of C9 to the π^* orbitals of the C8−O5 and C7−O4 bonds are almost the same (150.94 and 151.45 kcal/mol, respectively), the stabilization energies of σ donation from O5 and O4 to the copper center are significantly different (53.34 and 46.08 kcal/mol, respectively). In trying to complete its fourth coordination by approaching the C5−O2 bond, Cu has to weaken one of its coordinations, namely O4, which results in an increase in bond length. The geometry of the Cu(I) center in **E1** is far from that of the ideal tetracoordinated copper complexes.[20] The C4−C5−O4−O5 dihedral angle is 139.7° and it reaches an almost ideal geometry in the product by increasing to 174.5°.

If a free ylide, instead of a copper-stabilized one, were present, O2 would be attacking C3 to form a ring in the transition state, which would lead to the formation of a double bond between C4 and C5. In **TS-E1**, the interaction between copper and the C5−O2 bond vanishes in the cyclization stage. The C4−C5 bond becomes an attractive center for copper to participate in π back-donation, due to its olefinic nature. The sum of stabilization energies of the σ and π donation of this bond to copper lone pairs is 69.71 kcal/mol. Back-donation from copper to this bond (46.66 kcal/mol) appears as a stabilizing interaction in the transition state, which was not present in **E1**. Thus, the C4−C5 bond shortens slightly (1.493 Å in **E1** and 1.477 Å in **TS-E1**) and converges to the carbon−carbon bond length of a typical aromatic ring in the final product. The low barrier of cyclization (Figure 3) and the resemblance of the geometry of the transition state **TS-E1** to that of **E1** (Figure 2) indicate the presence of an early transition state.

In the product of **E1**, **P-E1**, the new bond is between the O2 and C3 atoms, forming the dioxole ring. Although the partial charges on the ring atoms showed some small changes, on the average, the total charges of the ring atoms are almost the same before and after the ring closure (−0.17, −0.21, and −0.23 in **E1**, **TS-E1**, and **P-E1**, respectively). The conformational changes due to dioxole ring formation are minimal. The angle between the acac and the dioxole ring planes is 115° in **P-E1**.

In Figure 3, the relative energies of the ylides **E1**−**E3**, the transition states obtained from them, and the products are given. The full set of energy values used to calculate the Gibbs free energies of the molecules is given in Table 1. The free energies of activation are 1.8, 2.9, and 2.4 kcal/mol for **E1**−**E3**, respectively. **E1** has the lowest energy, and its energy is only 0.8 kcal/mol lower than that of the next nearest (*E*)-ylide conformer, namely **E2**. Two conformers other than the global minimum are considered in modeling the reaction coordinates because, first, those conformers have very similar energies and, second, experimentally two isomers of dioxoles were observed but not isolated. According to our calculations, these two isomers would be **P-E1** and **P-E2/P-E3**, which correspond to two different modes of ring closure reactions leading to dioxole products, depending on the attacking side of the carbonyl oxygen. This attack may take place either above (**TS-E1**) or below (**TS-E2** and **TS-E3**) the enone plane. Thus, the sterically less hindered cyclization, through **TS-E1**, is more favored than that through **TS-E2** and **TS-E3**. Boltzmann distributions of the reactants at the reaction temperature (353 K) show that 72.6% **E1**, 23.2% **E2**, and 4.2% **E3** are expected to be present in the reaction mixture. By assuming that the amount of **E3** is negligible compared to that of **E1** and **E2**, the ratio of the rate constants of the dioxole formation reactions is calculated from the activation energies of cyclizations of **E1** and **E2**, by employing the Arrhenius equation at 353 K, and found to be 78:22. It should be noted that **P2** and **P3** are rotamers and can be transformed into each other by a free rotation around the single bond C4−C6. As a result, the final products are estimated to be **P-E1′** and a mixture of **P-E2′** and **P-E3′**, which may correspond to the experimentally observed ratio of 75:25. The final products (**P-E1′** and **P-E2′**/**P-E3′**) are formed after the regeneration of the catalyst by the reagents in the reaction medium, such as solvent, diazomalonate, unreacted substrate,

(20) Padwa, A.; Austin, D. J. *Angew. Chem., Int. Ed. Engl.* **1994**, *33*, 1797−1815.

Molecule	Electronic Energy (in au)	Thermal Correction to Gibbs Free Energy(in au)	Sum of electronic and thermal Free Energies (in au)	Relative Gibss Energy(in kcal/mol)
N_2	-109.5241291	-0.0128510	-109.5369800	
2	-1985.4949914	0.0788710	-1985.4161210	
3	-604.5002282	0.0813540	-604.4188740	
5	-386.0662750	0.1316810	-385.9345940	
E1	-2866.6175213	0.3295920	-2866.2879290	-34.7
TS-E1	-2866.6167545	0.3317300	-2866.2850240	-32.9
P-E1	-2866.6416834	0.3336450	-2866.3080380	-47.3
E2	-2866.6163696	0.3293850	-2866.2869840	-34.1
TS-E2	-2866.6140465	0.3316510	-2866.2823950	-31.2
P-E2	-2866.6417247	0.3337230	-2866.3080020	-47.3
E3	-2866.6143117	0.3293650	-2866.2849470	-32.8
TS-E3	-2866.6126159	0.3316030	-2866.2810130	-30.4
P-E3	-2866.6417418	0.3336590	-2866.3080830	-47.4

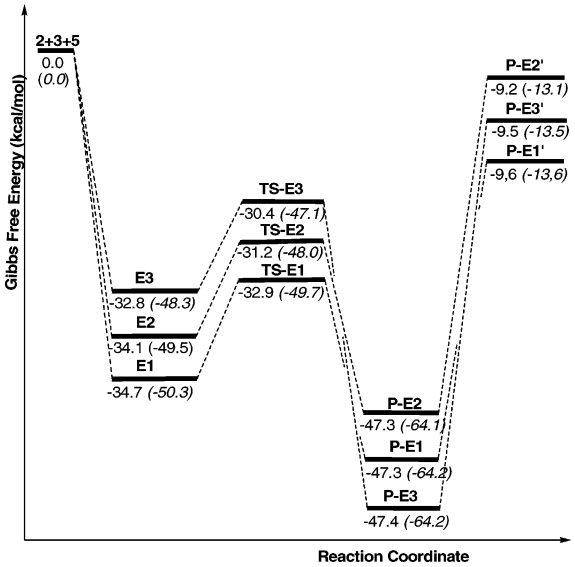

Figure 3. Gibbs free energy diagram (at 298 K in kcal/mol) of 1,3-dioxole formation. The values given in parentheses are the zero-point corrected electronic energies.

Table 1. Full Set of Energy Values Calculated by B3LYP/6-31G*[a]

molecule	electronic energy (au)	thermal cor to Gibbs free energy (au)	sum of electronic and thermal free energies (au)	rel Gibbs energy (kcal/mol)
N_2	−109.524 129 1	−0.012 851 0	−109.536 980 0	
2	−1 985.494 991 4	0.078 871 0	−1 985.416 121 0	
3	−604.500 228 2	0.081 354 0	−604.418 874 0	
5	−386.066 275 0	0.131 681 0	−385.934 594 0	
E1	−2 866.617 521 3	0.329 592 0	−2 866.287 929 0	−34.7
TS-E1	−2 866.616 754 5	0.331 730 0	−2 866.285 024 0	−32.9
P-E1	−2 866.641 683 4	0.333 645 0	−2 866.308 038 0	−47.3
E2	−2 866.616 369 6	0.329 385 0	−2 866.286 984 0	−34.1
TS-E2	−2 866.614 046 5	0.331 651 0	−2 866.282 395 0	−31.2
P-E2	−2 866.641 724 7	0.333 723 0	−2 866.308 002 0	−47.3
E3	−2 866.614 311 7	0.329 365 0	−2 866.284 947 0	−32.8
TS-E3	−2 866.612 615 9	0.331 603 0	−2 866.281 013 0	−30.4
P-E3	−2 866.641 741 8	0.333 659 0	−2 866.308 083 0	−47.4

[a] Gibbs free energies are calculated at 353 K.

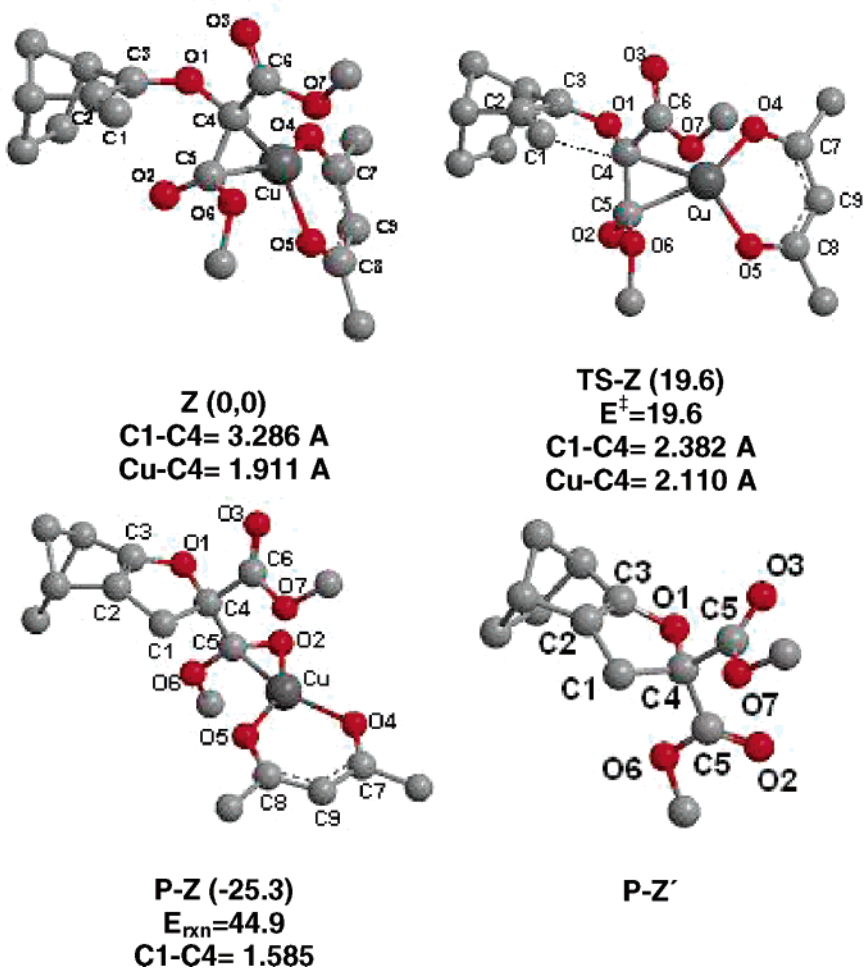

Figure 4. Optimized geometries of the (*Z*)-ylide (**Z**) its transition-state geometry (**TS-Z**), and the product (**P-Z**). Relative electronic energy differences with respect to **Z** (in parentheses), activation energies ($E^{\ddagger}$), and reaction energies (E_{rxn}) are given in kcal/mol; bond distances are given in Å.

and the bidentate ligand. However, those steps have not been considered in calculations, since cyclization of the metal-stabilized ylide **E** is the critical step in explaining the experimentally observed selectivity.

The single-point energies of the species along the dioxole formation path have also been calculated by a different functional with the same basis set (B3PW91/6-31G*) and the same functional with a higher basis set (B3LYP/6-311+G**) in order to test the level of the methodology. These functionals or basis sets have given slightly higher or lower energy differences; however, the order of the activation barriers and the relative stabilities did not show any significant change.

2. Alternative Cyclization Reaction Starting from the Carbonyl Ylides: Dihydrofuran Formation. Various α,β-unsaturated carbonyl compounds with the same[6−8] or different metal catalysts[4] gave the dihydrofuran derivatives as products. To complete the overall picture of the cyclization reactions of carbonyl ylides in the presence of copper catalysts, modeling of an alternative path leading to the dihydrofuran product was necessary for our purposes.

This alternative cyclization reaction starting from the carbonyl ylide is only possible if the reaction proceeds through the (*Z*)-ylide, since (*E*)-ylides require a free rotation around the carbonyl group of the substrate (C3═O1 group (Scheme 2)). In this mechanism, the product is formed by the attack of the carbene carbon at the olefinic carbon (C1 in Figure 4). In Figure 4, the lowest energy conformer of the **Z** ylide, its transition-state geometry, and the product are given.

The **Z** ylide given here has the lowest energy among its conformers considered, due to the less steric crowding of the methylene esters on the bicyclic side. The Cu center approaches one of the ester sites and completes its coordination by coordinating to the carbonyl carbon, where the Cu−C5 bond is 2.099 Å. The NBO analysis of **Z** has shown that the stabilization energy of σ donation from C5−O2 to Cu is 9.25 kcal/mol, whereas that of π-back-donation from Cu to C5−O2 is 22.64 kcal/mol. The π back-donation in **Z** is approximately 4 kcal/mol higher than that of in **E1**, and this is reflected in the C5−O2 bond lengths as 1.223 Å in **Z** and 1.243 Å in **E1**. NBO analysis reveals that there is no back-donation from copper metal to acac in **Z**, the same as in **E1**, since oxygen ligands are known to be poorer π acids compared to bidentate or tridentate σ and π donor nitrogen ligands, which are strong π acids with a high back-bonding capability.[13a] As the cyclization reaction proceeds, C4 approaches C1 and, as a result, the Cu−C4 bond lengthens in **TS-Z**. However, the Cu−C5 bond, which is necessary for copper's fourth coordination, does not show a change in distance from **Z** to **TS-Z**. This has also been demonstrated by the donor−acceptor relationships in the NBO analysis. In **Z-TS**, σ donation from C5−O2 to Cu and π back-donation from Cu to C5−O2 have shown similar values for **Z** and **TS-Z** (9.66 and 22.38 kcal/mol in **TS-Z**, respectively). The dihedral angle O1−C4−Cu−O4 changes from 39.8° in **Z** to 44.4° in **TS-Z**. By this change in dihedral angle copper compensates the coordination that it loses from C4 by attracting one of the lone pairs of ester oxygens and coordinating with O7. Thus, the Cu−O7 distance

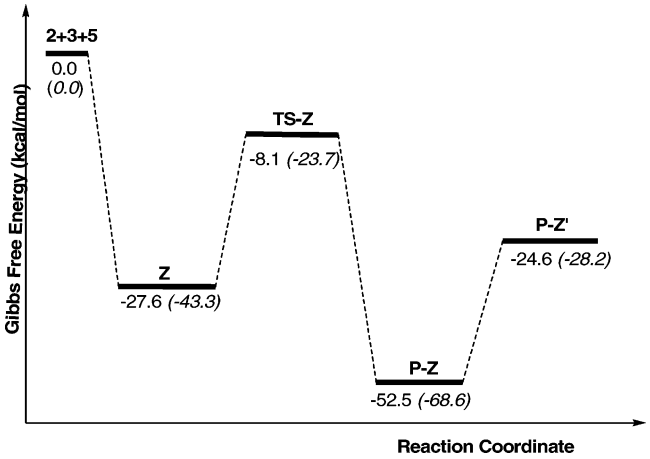

Figure 5. Gibbs free energy diagram (at 298 K in kcal/mol) of dihydrofuran formation (B3LYP/6-31G(d)). The values given in parentheses are the zero point corrected electronic energies. Energies are not to scale.

decreases from 3.095 Å in **Z** to 2.432 Å in the transition state. In **TS-Z**, the distance between the reacting centers C1 and C4 is reduced to 2.382 Å and this newly forming bond stabilizes the π^* orbitals of C5−O2 and C6−O3 by 151.0 kcal/mol. The dramatic decrease in the partial charge on C4 (0.29− in **Z** and 0.08− in **TS-Z**) makes it a more a reactive center for the nucleophilic attack of C1. The reduced electron density on C4 is delocalized on the carbonyl moiety of the ester groups. Furthermore, the σ^* orbital of the new C1−C4 bond is stabilized by the delocalization energy, which is 20.79 kcal/mol, coming from the π orbital on the C2 and C3 atoms. These donor−acceptor interactions facilitate C1−C4 bond formation. While C1 and C4 are approaching each other, C2−C3 bond turns into a double bond by shrinking from 1.464 Å to 1.380 Å.

In structures where copper coordinates to three sites, effective population of the copper d^{10} shell by groups or atoms in its vicinity is mandatory. Thus, in the structures we have considered, copper binds to C5 in **Z** and O7 in **TS-Z**. This fourth coordination can be fulfilled by an intermolecular host, such as solvent or any other reagents in the reaction medium. However, we have not considered this effect in our calculations, since an intramolecular coordination is energetically and entropically favored in general and also considering intermolecular assistance would be computationally expensive. Furthermore, the fourth coordination (Cu−C5) is present in both **Z** and **TS-Z** structures, which does not make a dramatic change in the overall reaction barrier.

After the ring closure takes place, the two rings, acac and dioxole, are oriented parallel to each other in **P-Z**. The acac ring that is stabilized by electron delocalizations distances itself from the remaining part of the molecule. As C4 attacks C1 in the cyclization reaction, Cu−C4 coordination is broken, which is compensated by attack at the carbonyl oxygen atom, O2, in **P-Z**. This causes a dramatic change in the dihedral angle of O5−Cu−C4−C5 from −14.2° in **TS-Z** to −113.8° in **P-Z** and a decrease of 0.12 Å in the Cu−C5 distance. The new coordinating olefinic site has a strong stabilization (75 kcal/mol in **P-Z)** from the metal's lone pairs to the π^* molecular orbital localized on C5−O2, which was originally 15 kcal/mol in the transition state (**TS-Z**). In Figure 5, the Gibbs free energy diagram of the dihydrofuran formation reaction is given. **P-Z** is the product before the metal catalyst is regenerated. **P-Z′** is the final product (**6**) of the reaction.

3. Comparison of the Competing Reaction Mechanisms. The calculations have demonstrated that, with the concerted mechanism, (*E*)-ylide gives only the 1,3-dioxole, whereas the dihydrofuran derivative formation is possible only through the (*Z*)-ylide. In the latter mechanism, the C1−C2 double bond (Figure 4; **Z**) must lose its olefinic character and rotate so as to bring the reacting centers close to each other for an efficient overlap. The reacting center, C4, is at the center of two ester groups that have an extended delocalization; thus, it will resist pyramidalization as it undergoes reaction. Additionally, ester groups will cause steric hindrance in the vicinity of reacting centers. In **TS-Z**, the interaction between Cu and the carbene carbon (C4) weakens and also the acac ring orients itself to a more planar position, allowing effective delocalization between the Cu and the acac groups as the dihyrofuran formation proceeds. These geometric hindrances in the reactant cause an increase in the reaction barrier and make the reaction difficult.

The transition state in dioxole formation is very early, which results in a low barrier for the reaction. The reacting centers are oriented in a very favorable geometry for an efficient overlap in cyclization to a dioxole product. Cyclization in **TS-E1** is not hindered by steric or pyramidalization effects. Thus, cyclization to dioxole products does not require a dramatic change in the overall geometry of the reactant, which results in a much lower barrier.

The back-donations also aid in facilitating the dioxole formation. In **TS-E1**, σ and π back-donations from the metal to the C5−O2 bond vanish, while the stronger σ and π back-donations from the metal to the C4−C5 bond persist. This weakens the C5−O2 bond and sets O2 free to attack at the C3 atom, the only nucleophilic center on the substrate side. On the other hand, in **TS-Z**, there is no such back-donation from the metal to the C4−C5 bond to stabilize the transition-state geometry.

The σ donations and π back-donations calculated by NBO analysis demonstrated the importance of stabilizations coming from the metal and their effects on the activation barriers. In **TS-E1**, the bond between C4 and C5 gains a double-bond character, which allows copper to coordinate strongly by π back-donations from the metal to the olefinic site, which has not been observed in **E1**. The acac ring does not undergo a dramatic change in its three-dimensional orientation with respect to copper in **TS-E1**. These effects decrease the activation barrier leading to the 1,3-dioxole product.

4. Conclusions

The Cu(II)-catalyzed reaction of **5** with **3** gave the 1,3-dioxole product **7**. The computational studies confirmed this observation by modeling both dioxole- and dihydrofuran-forming reaction pathways. Reaction of **4** with **5** can yield the ylide intermediate in one of the two possible geometries, namely *E* and *Z*, depending on the orientation of the substrate. The transition states and the activation barriers for the possible ring closure paths starting from the (*E*)- and (*Z*)-ylides were studied to understand the reaction mechanism and the factors affecting it.

The product distribution of this reaction depends on the relative thermodynamic stabilities of the (*E*)- and (*Z*)-ylides and the rotational barrier between them. Dihydrofuran products can only be obtained if the (*Z*)-ylide's energy is lower or comparable to the energy of the (*E*)-ylide. The interconversion between (*E*)- and (*Z*)-ylides depends on the strength of the carbonyl bond of the substrate and is facilitated if the rotation is not hindered sterically and this bond is weakened. Recently, it has been reported that the addition of a vinyl group to an acetaldehyde oxide weakens the C═O bond, making rotation about this bond possible and also lowering the rotation barrier by 8−12 kcal/

mol.[21] Here, the rotation around C3−O1 bond is sterically hindered and it is not possible to generate different ylides as starting conformers.

This is the first computational and experimental study of cyclization reactions leading to dioxole or dihydrofuran type products where $Cu(acac)_2$ is used as a catalyst in diazo decomposition. According to our previous experiments,[7,8] formation of a dioxole type product is not expected initially in this reaction. This result can be attributed to the fact that the previous ketonic structures[6−8] have a rotatable single bond between the C═O and C═C moieties but the ketone substrate in this study has a very rigid bridged cyclic structure that prevents a free rotation around the single bond C2−C3, which in turn relieves steric hindrance present in the carbonyl ylides. We conclude that the nature of the substrate and the stability of the carbonyl ylide are the dominant factors in determining the product distribution.

Our theoretical results are in good agreement with the experimental results, in which the only characterized products are the dioxole derivatives in a ratio of 75:25 for **7a** and **7b**. The calculated ratio of **P1** to **P2** is found to be as 78:22, and the experimentally observed products **7a** and **7b** are estimated as **P1** and (**P2**/**P3)** isomers.

IV. Experimental Section

1. Experimental Details. Reagents were of commercial quality, and reagent-quality solvents were used without further purification. Dimethyl diazomalonate (**3**; dmdm) was prepared according to literature procedures. IR spectra were determined on a JASCO FT-IR 5300 spectrometer. ^{1}H NMR: 250 MHz Bruker aparatus, in $CDCl_3$, TMS as internal standard, δ in ppm, J in Hz, at 25 °C. ^{13}C NMR: at 60 MHz. GC/MS: Hewlett-Packard instrument with HP-1 capillary column (24 m, packed with cross-linked (phenylmethyl)-siloxane; column conditions: isothermal at 150 °C for 7 min, then heating to 280 °C at a rate of 5 °C/min, 0.54 bar of He, EI detector; t_R in min. MS: VG-Zapspec double-focusing spectrometer; EI at 70 eV; CI in isobutane. TLC was carried out on aluminum sheets precoated with neutral aluminum oxide $60F_{254}$ (Merck).

2. Reaction of 3-Methylene-2-norbornanone (5) with dmdm (3). A solution of 20 mmol of dmdm in benzene (4 mmol/1 mL) was added very slowly to a refluxing benzene solution of 30 mmol of the 3-methylene-2-norbornanone (2 mmol/1 mL) and 0.14 mmol of $[Cu(acac)_2]$ under N_2. Consumption of dmdm was monitored by IR. After the complete disappearance of the band at 2130 cm^{-1}, the mixture was filtered (gravity), and the solution was passed rapidly through a short column of neutral aluminum oxide to remove highly colored impurities and the catalyst. The GC-MS analysis of the crude mixture contained two products in a ratio of 75:25, with identical mass spectra, along with some unreacted enone. The crude reaction mixture was purified by preparative TLC (2:0.7 CCl_4−ethyl acetate on neutral aluminum oxide), giving product **7** as an isomeric mixture, along with some unreacted enone, which did not interfere with the signals of the products.

7a (isomer I, 25%): t_R = 10.4; EI-MS m/z 252 (M^+, 30), 224 (5), 193 (30), 176 (10), 165 (18), 137 (100), 105 (50).

7b (isomer II, 75%): t_R = 10.8; EI-MS m/z 252 (M^+, 35), 224 (40), 192 (100), 165 (20), 137 (30), 113 (20), 77 (20), 59 (20).

^{1}H NMR: 4.97 (bs, 1H, for **7b**), 5.28 (bs, 1H, for **7a**), 4.70 (bs, 1H, for **7b**), 4.62 (bs, 1H, for **7a**), 3,84 (s, 3H), 3.78 (s, 3H), 2.91 (bs, 1H), 2.26 (bs, 1H), 1.9−1.6 (m, 6H).

^{13}C NMR: 165.8, 164.3, 149.0, 106.9, 75.2, 67.0, 52.9, 49.0, 45.0, 39.5, 36.5, 25.2, 22.4.

Acknowledgment. We gratefully acknowledge the ITU High Performance Computing Center for the computer time provided, TUBITAK for the grants 105E067 and 105T395, and also the ITU Research Fund for supporting the projects 31555 and 31087.

Supporting Information Available: Tables and figures giving Cartesian coordinates of all reported structures, number of imaginary frequencies, and total electronic and zero-point vibrational energies as well as Gibbs free energies, NBO charges, relevant bond distances, bond angles, and dihedral angles of all of the structures discussed in the paper, single-point energies calculated by different functionals and basis sets, and NMR spectra. This material is available free of charge via the Internet at http://pubs.acs.org.

OM0609970

(21) Kuwata, K. T.; Valin, L. C.; Converse, A. D. *J. Phys. Chem. A* **2005**, *109*, 10710−10725.